

Supplementary Material

1 SUPPLEMENTARY METHODS

1.1 TC recruitment

Under non-inflammatory conditions, it was assumed that TC entry and exit remain constant and TCs occupy a constant percentage (55%) of the total paracortical volume. The model represents a LN of 0.113-0.268 mm³, implying a LN mass of 0.18-0.44mg (based on collaborative unpublished measurements of murine popliteal LN mass versus volume). Reported lymphocyte recruitment for a popliteal LN of 1.15g is 4x10⁷ lymphocytes/hour and up to 40% of lymphocytes are B cells (Cahill et al., 1976; Habenicht et al., 2016; Battaglia et al., 2003). The model represents half a paracortex, therefore TC recruitment rate was estimated as 1950-9000 TCs/hour under non-antigenic conditions. Naive TC transit time through the LN (T_{res}) was estimated as 6-24 hours (Tomura et al., 2008).

1.2 Agents and agent migration

The agents were designated as members of the TC or DC class (Figure S1). Simulated DCs appear in the paracortex at a constant entry rate for 2 days, subsiding over the following 12 hours. Entry rate of DCs was scaled from counts of migrating DCs and initial TCs in a murine LN post-immunisation, with DCs totalling 4% of cells present (Acton et al., 2014). TC migration was assumed to follow a random walk with pauses. Previous models have described TC migration with Brownian motion, a random-walk with persistence, run and tumble, and Lévy walks amongst other methods, partly due to differing reports of *in-vivo* migration. (Celli et al., 2012; Bogle and Dunbar, 2008; Brown et al., 2018; Harris et al., 2012).

1.3 Agent interaction and signal integration

During TC-DC interaction, TCs remain stationary. Antigenic signal is presented by the DCs in the form of representative values of MHC I or MHC II, and decays with time (t) with the form :

$$MHC\text{I}(t) = MHC\text{I}_i(0.5)^{\frac{t}{MHC\text{I}t_{1/2}}} \quad (\text{S1})$$

$MHC\text{I/II}_i$ is initial MHC I or MHC II presented with estimated MHC half-lives $MHC\text{I}t_{1/2}$ and $MHC\text{II}t_{1/2}$. During cognate TC-DC interaction, CD4⁺/CD8⁺ TCs gain (S) at a rate proportional to the MHC I or MHC II signal respectively (Figure 2.C). Accumulated stimulation decays at a constant rate. Total change in TC stimulation is therefore given according to the first order rate equation:

$$\frac{dS}{dt} = K_s MHC\text{II}(t) - \lambda_S S(t) \quad (\text{S2})$$

Where K_s is a rate constant and λ_S is a decay factor. Accumulated simulation decays to a minimal value of S=1 to allow differentiation between cognate TCs that gain and lose simulation (S=1) and those that never gain simulation (S=0). Probability of cognate CD4⁺ activation (P_{a4+}) or cognate CD8⁺ activation (P_{a8+}) is calculated with a sigmoidal function given by:

$$P_{a4+} = \frac{1}{1 + e^{\frac{-S - Act\mu_4}{Actl_4}}} \quad (\text{S3})$$

Parameter $\text{Act}\mu_4$ determines the value of S required for 50% probability of activation and $\text{Act}\ell_4$ determines steepness of sigmoid inflection (Figure 2.D). Activation probability for CD8⁺ TCs (P_{a8+}) is determined with a sigmoid curve using a lower inflection point, ($\text{Act}\mu_8$), than for CD4⁺ TCs, unless the interacting agDC is licensed (see 2.4). Model parameters were estimated such that TC activation became apparent 8-15 hours post DC-arrival (Hugues et al., 2004; Mempel et al., 2004; Stoll et al., 2002). This method of signal integration and the subsequent progressive patterns of TC proliferation and differentiation is supported by *in-vivo* observations and modelling descriptions (Stoll et al., 2002; Germain and Stefanová, 1999; Rachmilewitz and Lanzavecchia, 2002; Lanzavecchia and Sallusto, 2002). It is assumed that co-stimulatory requirements are met as agDCs are highly efficient antigen-presenting cells.

Post-activation, proliferation is possible every 11 (CD4⁺) or 9 (CD8⁺) $\pm 1\text{hr}$ (De Boer et al., 2003; Foulds et al., 2002; Nelson et al., 2015; Tubo et al., 2013). Differentiation into effector or memory cells is possible after $>=4$ divisions, with differentiation probability determined with a second set of sigmoidal probability curves with midpoint $\text{Dif}\mu_{4+}$ and $\text{Dif}\mu_{8+}$ respectively (Miller et al., 2002; Linderman et al., 2010). Greater CD4⁺ TCs dependence on continued stimulation for differentiation than CD8⁺ TCs was implemented by using a higher minimum threshold of accumulated stimulation for CD4⁺ differentiation than for CD8⁺ TCs (Schrum et al., 2005; Wong and Pamer, 2001; Kaech and Ahmed, 2001; van Stipdonk et al., 2001; Shaulov and Murali-Krishna, 2008). Effectors TCs that underwent < 8 proliferations were less likely to differentiate into memory cells than those that underwent >8 proliferations. This was implemented by assigning differentiation ratios of $\text{dif}_{\text{early}}$ and dif_{late} to the two different subsets ($<=8$ or >8 divisions).

During TC activation and proliferation, S1P₁r expression was estimated from several *in-silico* studies. Expression change was considered following TC migration velocity into areas of high S1P concentration, changes in TC egress from the LN and changes in S1P₁R expression relative to naive S1P₁r expression following TC activation and with subsequent proliferation (Figure 2.F) (Pham et al., 2008; Matloubian et al., 2004; Garris et al., 2014).

2 SUPPLEMENTARY TABLES AND FIGURES

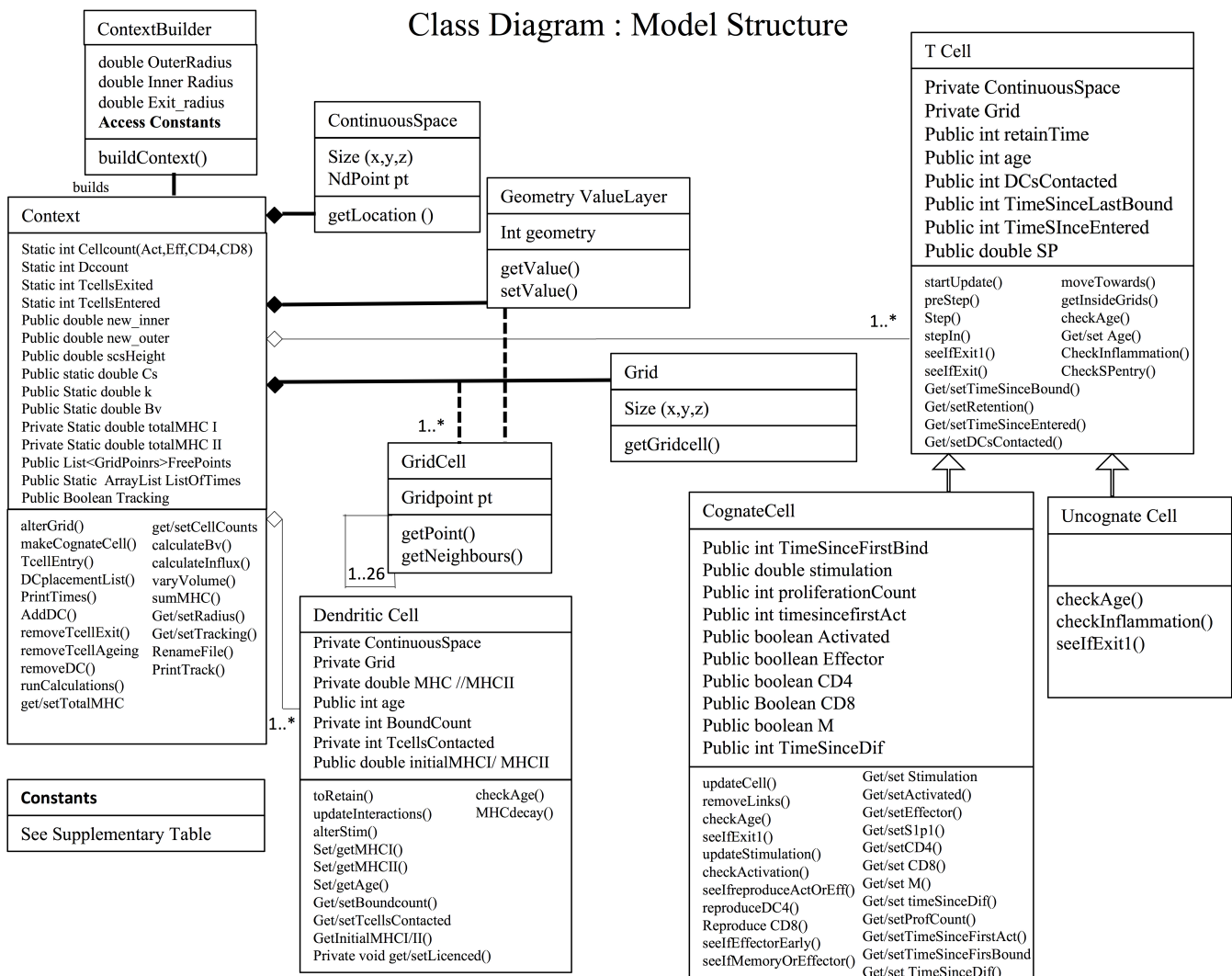


Figure S1. A class diagram displaying the underlying ABM structure. The model is constructed using instructions in the 'context builder' class. The entire modelling domain is described by the context class, and each compartment of the domain is described by the GridCell class. In a 3D simulation, each grid cell can be queried to identify the 26 neighbouring grids and how many agents they contain. The TC class is a template for the T cell object produced and is instantiated thousands of times to create T cells with the same variables but slightly different values. A subclass of cognate T cells extends the template to contains more methods and variables relating to interaction and proliferative response.

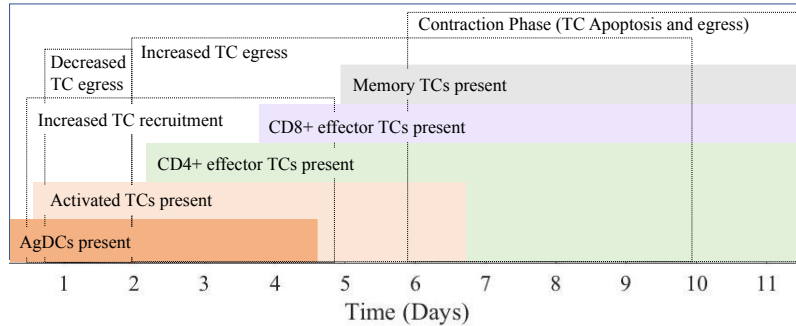


Figure S2. Captured phases of TC trafficking and response to AgDC stimuli. Changes in proliferation and differentiation continued after the initial stimulus was no longer present. TC recruitment and TC egress changes also accompanied the response.

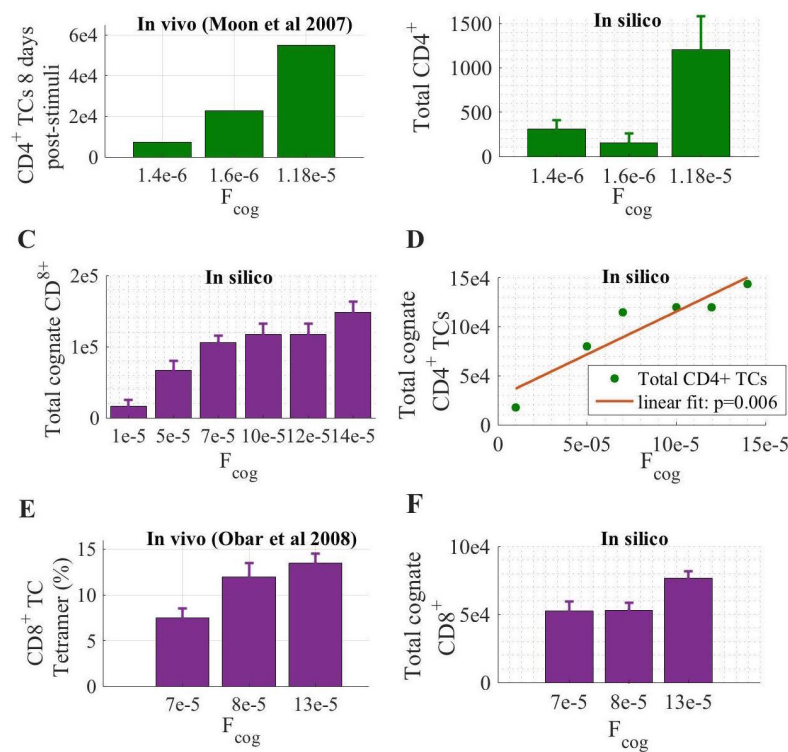


Figure S3. TC responses in-silico and in-vivo when proportion of cognate TCs was varied. A. $CD4^+$ magnitude of response in dLNs of mice to injected antigen correlated to starting estimated frequency of cognate TCs in a sample of 1×10^7 TCs. B. Results in-silico showed an overall increase in response with increasing F_{cog} ($n=8$). Simulations using a wider range of F_{cog} values (C,D) confirmed no. of total cognate $CD4^+$ TCs and $CD8^+$ TCs increased linearly with F_{cog} . E. Mice were infected with VSV-M45 or VSV-ova with starting precursor $CD8^+$ frequencies of 7×10^{-5} , 8×10^{-5} and 13×10^{-5} respectively. The peak number of resulting TCs as a percent of overall $CD8^+$ TCs present is shown. F. Simulations using the same F_{cog} in-silico showed a similar increasing trend with similar increase rate.

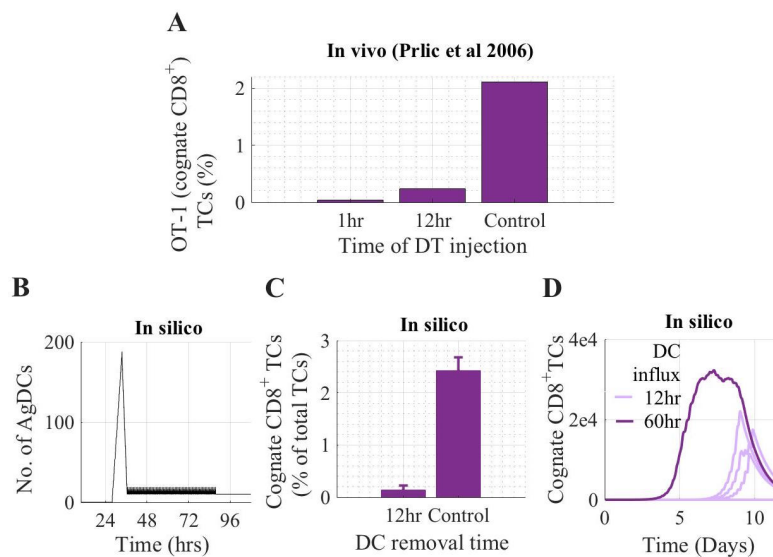


Figure S4. TC responses in-silico and in-vivo when a stimulus is abruptly abolished. A. Transgenic Rats were used that would eliminate specific injected agDCs when the rat was injected with DT within 12 hours. The rats were injected with OT-1 CD8⁺ TCs specific for agDCs that were subsequently injected. DT was then injected at 1h, 12 and 48hr(not-shown) later, curtailing the time that the agDCs would normally spend in the LN. Adapted from Prlic et al 2006. B. The simulated disrupted input stimuli achieved by curtailing the 60hr DC influx at 12+-2hr. C-D. The results of simulations (n=8). Mean (+SEM) CD8⁺ TCs were reduced 91% when the stimulus was curtailed at 12hrs compared to sustained entry for 60hrs. D. individual CD8+ TC responses varied by a factor of 10 in an all or nothing response manner.

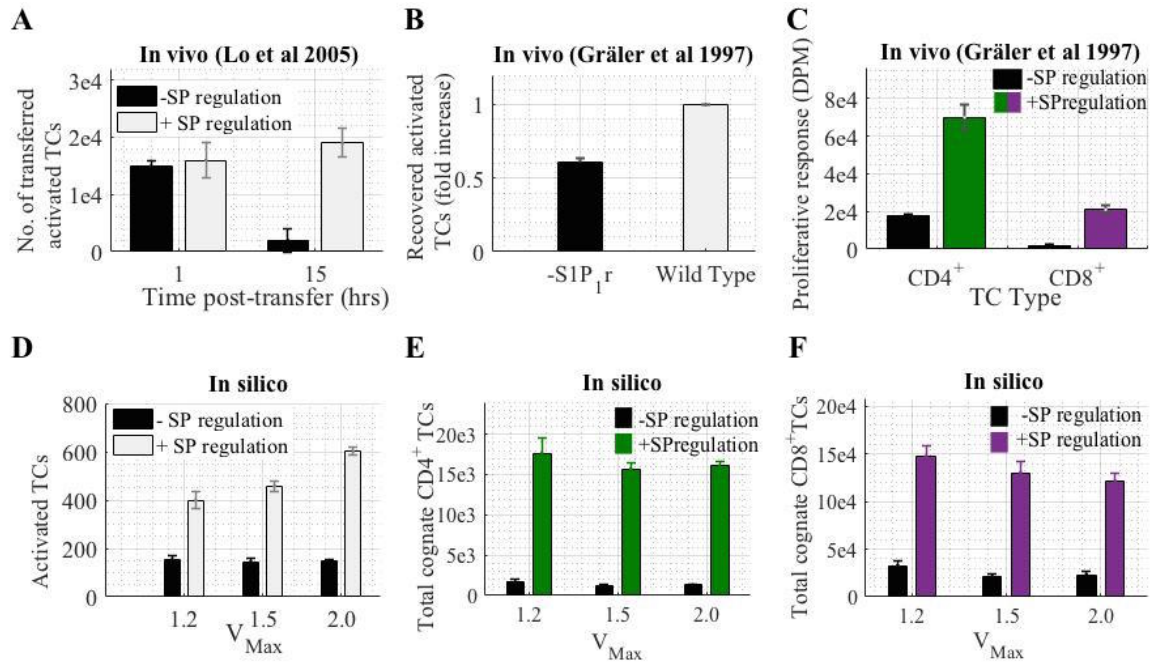


Figure S5. TC responses in-silico and in-vivo when S1P₁r down-regulation is inhibited. A. Pre-activated wildtype TCs (S1P₁r) and pre-activated TCs over-expressing S1P₁r (S1P₁r++) were transferred into mice and further entry of TCs was blocked. 15hrs later there was a 90% reduction in retention of S1P₁r++ activated TCs. Adapted from Lo et al 2005. B. The number of activated TCs in the LNs 24hours post-transfer dropped by 40% in transgenic mice with constitutive S1P₁r expression while (C) the proliferative CD4⁺ and CD8⁺ TC response decreased to 20% and 6% of that of the wild-type mice. Adapted from Gräler et al 1997. D-F. Simulation results (n=10) where S1P₁r down-regulation was prevented (-SP regulation), compared to baseline simulations (+SP regulation). Mean (+SEM) total number of activated TCs present was reduced 60%, 72% and 81% at V_{max}=1.2,1.5 and 2.0. E. The mean (+SEM) number of total CD8⁺ TCs, was diminished to 25,15 and 18% of control response at V_{Max}=1.2,1.5 and 2.0. F. CD4⁺ TCs were similarly diminished to 8-10% of control at all values of V_{max}.

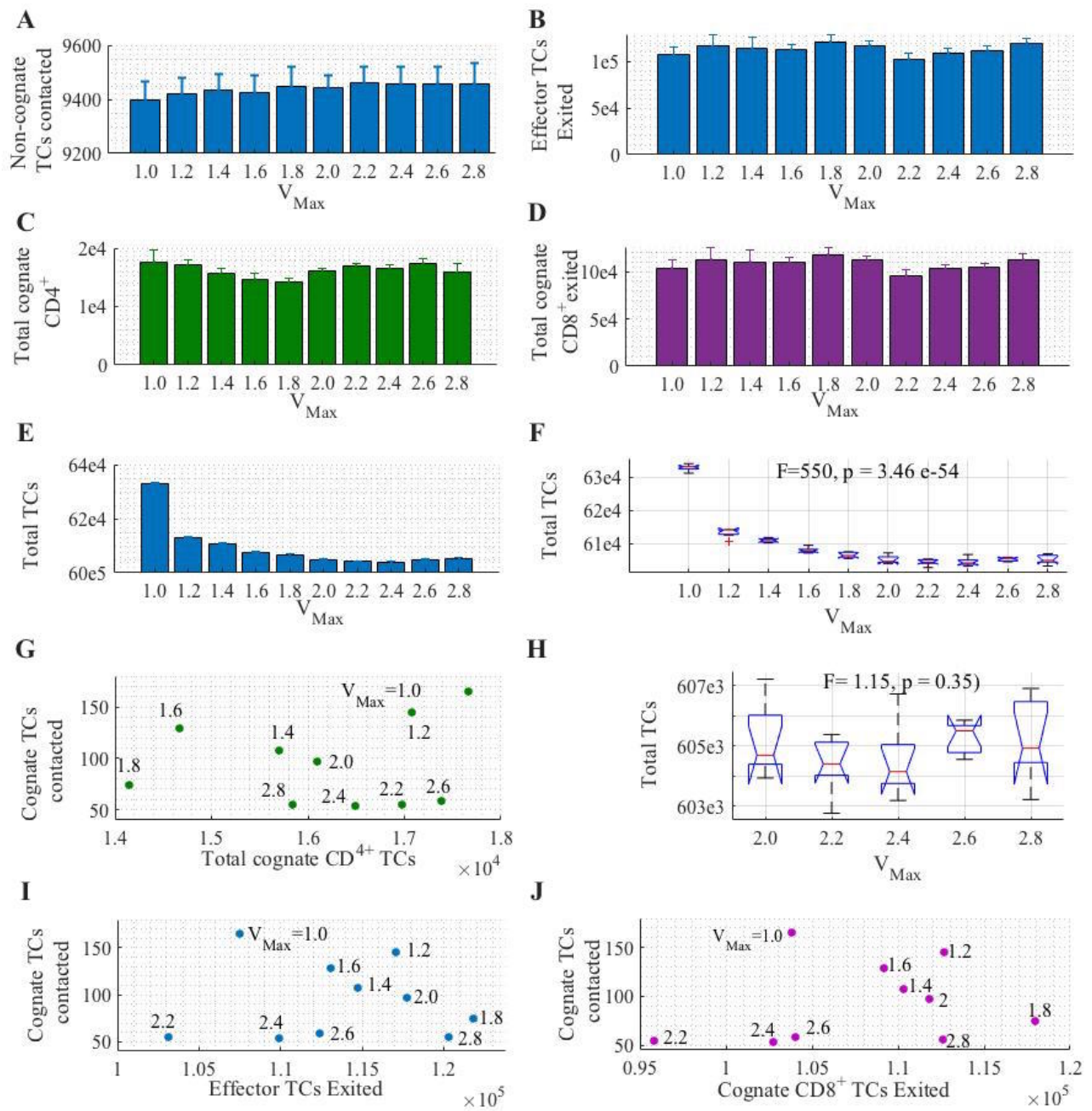


Figure S6. Additional data when V_{max} was varied with $T_{mid}=10e4$ TCs. A. The number of non-cognate TCs a DC contacted increased with LN swelling. B. No significant difference was apparent when effector TCs exited were plotted over time. C. Total cognate CD4⁺ TCs in the paracortex. D. Total CD8⁺ TCs that exited the paracortex. E,F. The total TCs present in the paracortex over the course of the simulation decreased as V_{max} increased, up to $V_{max}=2.0$ at which no further difference was observed (H). G, I, J. No correlation was observed between swelling, TC and DC contact and total cognate CD4⁺ TCs or Effector/cognate CD8⁺ TCs that exited by day 10.

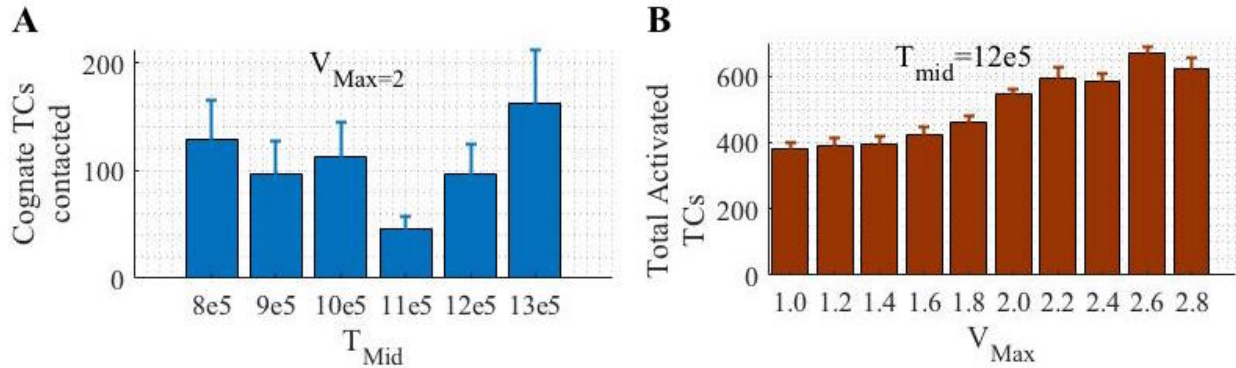


Figure S7. A. At $V_{max}=2.0$, no correlation between cognate TC and DC contacts and T_{mid} was observed. B. With a higher T_{mid} of 12e5, there remained a correlation between activated TCs and V_{Max} .

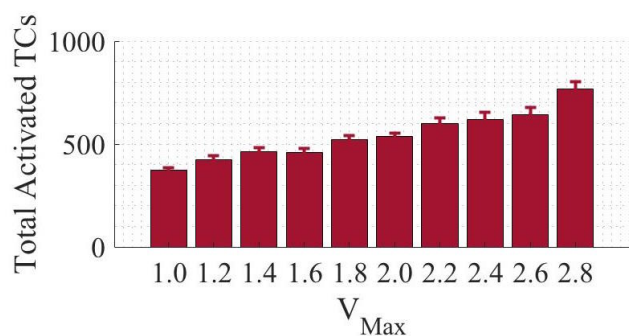


Figure S8. The activation of TCs at different maximal swelling when allowing TCs to return to HECs with a low probability increases with V_{max} ($p \cdot 10^{-5}$)

Table S1. Parameters that significantly influenced the number of effector TVs in the paracortex from day 3 to day 12 post-stimuli. There is a greater correlation between maximum CD8⁺ TC proliferation and effector TCs produced in the expanding paracortex than in the fixed volume paracortex. In an expanding paracortex there is also a negative correlation with TC recruitment, and maximal paracortical swelling in the second week of the simulation.

Parameter	Day 3	Day 4	Day 5	Day 6	Day 7	Day 8	Day 9	Day 10	Day 11	Day 12
Without Swelling										
Max_{P4+}							+		+	+
T_{short}					+					
Max_{NT}			+							
MHC_i					+					
F_{cog}	++	++	++	++	++	++	++	++		
ϕ_{DC}	++	++	++	++	++	++				
T_{DCin}	---	---	---	---						
SP_{early}	-									
With Swelling										
Max_{P8+}					+	++	++	++	++	++
Max_{P4+}					+					
T_{NC}								+	+	
T_{short}	+									
MHC_i								-		
P_{cog}	++	++	++	++						
ϕ_{DC}	++	++	+					-	-	
T_{DCin}	---	---	---	---	---	---	---			
SP_{early}	-									
R_F						-	--	--	--	--
V_{Max}	++		+	---	---	---	---	---	---	---
$0.05 > p > 0.001 = +/- \quad 0.001 > p > 10^{-6} = ++/- \quad 10e^{-6} > p > 0 = +++/-$										

Table S2. Parameters that significantly affected memory TCs number in the paracortex. Data is only shown from day 5 to day 12 post-stimuli, as they are not produced in the first few days. At day 5, V_{max} still showed some positive correlation with memory TCs present but by day 7 shows a negative correlation.

Parameter	Without Swelling				With Swelling			
	Day 5	Day 7	Day 9	Day 12	Day 5	Day 7	Day 9	Day 12
Max_{P8+}						++	++	+
$difflate$	++	++	++	++	++	++		+
γ			-		-			
F_{cog}	++	++	+		++			
ϕ_{DC}	++	++						
T_{DCin}	---	---			---	---		
R_F								
V_{Max}	N/A	N/A	N/A	N/A	+	-	---	---
T_{mid}		N/A	N/A	N/A	-			
$0.05 > p > 0.001 = +/- \quad 0.001 > p > 10^{-6} = ++/- \quad 10e^{-6} > p > 0 = +++/-$								

Table S3. Parameters that significantly affected the number of memory TCs exited in the paracortex from day 5 to day 12 post-stimuli.

Parameter	Without Swelling				With Swelling			
	Day 5	Day 7	Day 9	Day 12	Day 5	Day 7	Day 9	Day 12
TP_{4+}			+			+	+	
Max_{p8+}					-	--	--	--
dif_{early}	++				++			
dif_{late}	+++	+++	+++	+++	+++	+	++	+
T_{NC}							+	
K_S	+							
γ	--	--	-		--	--		
MHC_i						-	-	-
F_{cog}	+++	+++	++	++	+++			
ϕ_{DC}	--	--			--	--	--	--
T_{DCin}	--	--			--			
SP_{early}	--				--	-		
R_F					-	--	--	--
V_{Max}	N/A	N/A	N/A	(N/A)	--	--	--	--

0.05 > p > 0.001 = +/- 0.001 > p > 10^{-6} = ++/- - $10e^{-6} > p > 0$ = +++/- - -

Table S4. Parameters that were not varied in the global sensitivity analysis

Symbol	Parameter	Value	Reference
Model Geometry			
r^p	Initial paracortex radius	200 μm	
-	Entry radius	0.5 r^p	Mueller and Germain (2009); Kuka and Iannacone (2014)
-	Exit radius	0.07 r^p	
-	Sub-capsular Sinus Height	0.7 r^p	
-	Grid Size	6 μm	-
TC properties			
-	Initial occupation	55%	He (1985)
-	Ratio CD4 $^+$:CD8 $^+$	0.7:0.3	Mueller and Germain (2009); Kuka and Iannacone (2014)
-	TC naïve lifespan		Tough and Sprent (1995); Sprent and Tough (2001)
-	TC entry in afferent LVs to HEVs	0.1:0.9	Smith et al. (1970); Hall and Morris (1965)
Act_{4+}	Slope of CD4 $^+$ activation curve	-69.18	-
Act_{8+}	Slope of CD8 $^+$ activation curve	-80.71	-
Dif_{4+}	Slope of CD4 $^+$ differentiation curve	-17.26	-
Dif_{8+}	Slope of CD8 $^+$ differentiation curve	-13.58	-
β	Probability of movement	0.6	Park et al. (2010); Boscacci et al. (2010); Park et al. (2012); Girard et al. (2012); Miller et al. (2002)
P_e	Probability of egress	0.0126	-
γ	Max TCs per grid	2	-
T_{res}	TC residence time	24hrs	Catron et al. (2004); Tomura et al. (2008)
DC properties			
-	DC grid span	2 grids	Nitschké et al. (2012); Paharkova Vatchkova et al. (2004)
-	DC lifespan	2.5 days	Acton et al. (2014); Kamath et al. (2002); Bousso (2008)

Table S5. Parameters that were varied in the global sensitivity analysis.

Symbol	Parameter description	Default	Min	Max	Mean	SD	Distribution	Reference
TC response parameters								
Act μ_4	CD4* activation curve mean	120	70	230	-	-	Unif	Bajénoff et al. (2003); Yoon et al. (2007); Lawrence and Braciale (2004); Demotz et al. (1990); Lee et al (2002); Arens and Schoenberger (2010)
Act μ_8	CD8* activation curve mean	140	90	250	-	-	Unif	
Dif μ_4	CD4* differentiation curve mean	60	30	90	-	-	Unif	
Dif μ_8	CD8* differentiation curve mean	40	20	60	-	-	Unif	
TP ₄	Min. time between CD4* proliferations (hrs)	11	-	-	11	1.16	Norm	De Boer et al (2003); Nelson et al (2015); Foulds et al (2002); Tubo et al
TP ₈	Min. time between CD8* proliferations (hrs)	7	-	-	7	0.88	Norm	De Boer et al (2003); Foulds et al. (2002)
Max μ_8	Max proliferations CD8*	16	-	-	16	1.2	Norm	Butz and Bevan (1998); Murali-Krishna et al (1998); Busch et al. (1998); van Stipdonk et al. (2001)
Max μ_4	Max proliferations CD4*	10	-	-	10	1.2	Norm	Nelson et al. (2015); Tubo et al (2013); Foulds et al (2002)
Dif _{early}	Ratio of early differentiation into effector/memory TCs	0.01	0.001	0.02	0.01	-	Exp	William and Bevan (2004)
Dif _{late}	Ratio of late differentiation to effector /memory TCs	0.04	0.01	0.08	-	-	Unif	
TC interaction dynamics								
T _{NC}	Mean non-cognate T-DC interaction (min)	3.5	-	-	3.5	1	Norm	Bousso (2008); Miller et al (2004)
T _{Short}	Short cognate TC-DC interaction (min)	10.-15	-	-	10	3	Norm	Bousso (2008); Miller et al (2004); Mempel et al (2004)
T _{long}	Long cognate TC-DC interaction (min)	50.-70	-	-	50	12	Norm	von Andrian and Mackay (2000); Hugues et al. (2004); Mempel et al (2004); Stoll et al (2002)
T _{change}	Time TCs switch to long interactions (hrs)	8	-	-	8	1	Norm	
B _{Max}	Max TCs a DC can bind	3	1	5	-	-	Unif	
B _{Step}	Max TCs a DC can bind per step	15	4	20	-	-	Unif	Bousso and Robey (2003)
TC stimulation								
K _s	Stimulation gain coefficient	0.015	0.005	0.02	-	-	Unif	-
λ	TC stimulation decay factor	0.99	0.99545	0.9999	-	-	Norm	-
MHC _i	Initial MHC _i or MHCII	250	150	350	-	-	Norm	Cella et al. (1999); Kukutsch et al. (2000); Cella et al. (1997);
MHC _i _{1/2}	MHC _i half life (hrs)	19.7	-	-	19.7	6	Norm	Cella et al. (1999); Kukutsch et al.
MHCII _{1/2}	MHCII half life (hrs)	60	-	-	60	6	Norm	Cella et al. (1997); Baumgartner et al. (2010)
F _{cog}	Frequency of cognate TCs that enter	1.00E-04	5.00E-05	1.50E-04	-	-	Unif	Laouinin et al. (2000); Blattman et al. (2002); Nelson et al. (2015); Jenkins and Moon (2012)
ϕ_{DC}	Total DCs entering as % of initial TCs	0.04	0.02	0.06	-	-	Norm	Acton et al. (2014)
T _{DCin}	DC entry duration (days)	2.5	0.5	4.5	-	-	Unif	Acton et al. (2014)

Continued overleaf

Symbol	Parameter description	Default	Min	Max	Mean	SD	Distribution	Reference
	Sphingosine-1-phosphate receptor regulation							
SP _{entry}	S1P ₁ r expression post-entry	0.1	0.01	1	-	-	Unif	Pham et al. (2008), Matloubian et al. (2004), Lo et al. (2005)
SP _{act}	S1P ₁ r expression when activated	0.01	0.001	0.02	-	-	Unif	Pham et al. (2008), Matloubian et al. (2004), Lo et al. (2005), Garris et al. (2014)
SP _{early}	Effector S1P ₁ r expression (Proliferation>6)	0.8	0.3	1.3	-	-	Unif	Garris et al. (2014); Pham et al. (2008)
SP _{late}	Effector S1P ₁ r expression (Proliferation<=6)	0.4	0.01	1	-	-	Unif	
SP _{mem}	Memory S1P ₁ r expression	1	-	-	1	0.1	Norm	
SP _{IF}	S1P ₁ r on all TCs during inflammation	0.4	0.2	0.8	-	-	Unif	-
T _{Entry}	Time S1P ₁ r remains down-regulated post entry (min)	60	13	120	-	-	Unif	-
T _{Inflam}	Time to alter S1P ₁ r during inflammation (hrs)	4	1	7.5	-	-	Unif	-
	T cell recruitment							
RT1	Antigenic stim. threshold for TC recruitment increase (\sum MHCI)	2.00E+04	2.00E+04	1.00E+05	-	-	Unif	Hay and Hobbs (1977); Drayson and Smith (1981); Mackay et al. (1992); Webster et al. (2006)
RT2	Antigenic stim. threshold for TC recruitment increase (\sum MHCI)	4.00E+05	2.00E+05	2.00E+06	-	-	Unif	
R _F	Recruitment factor	3.00E-06	1.00E-06	4.00E-06	-	-	Unif	
	Paracortical expansion							
V _{Max}	Max fold-volume increase	1.00	2.00	2.50	-	-	Unif	-
<i>l</i>	Rate of volume change around m	7.00E-05	3.00E-05	1.00E-04	-	-	Unif	-
T _{mid}	No. of TCs present to reach 50% max volume	1.00E+05	9.00E+04	1.50E+05	-	-	Unif	-

2.0.1 UML diagrams

The following section presents the logic underlying the sub-methods that are called during the simulation. The order that each method is called is summarised in the previously shown 'Main' diagram (Figure 2B).

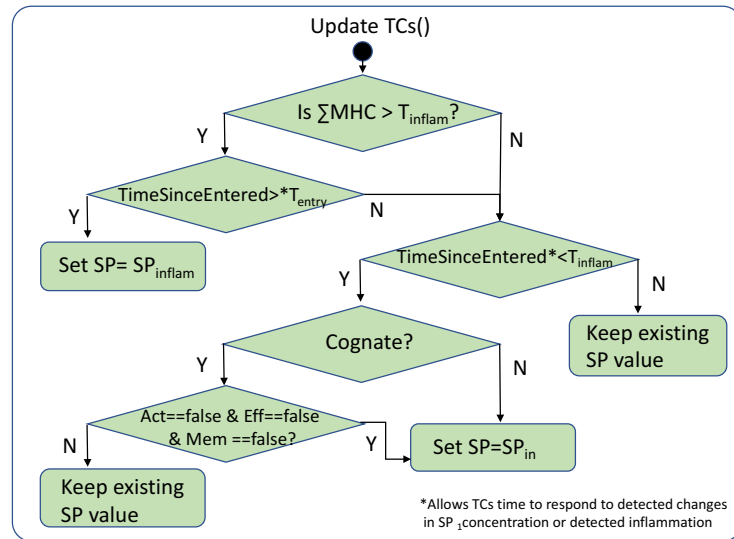


Figure S9. UML diagram for 'UpdateTCs'. By checking the time since the TC entered, a 'lag time' representing time for detection of signals and receptor internalisation to occur.

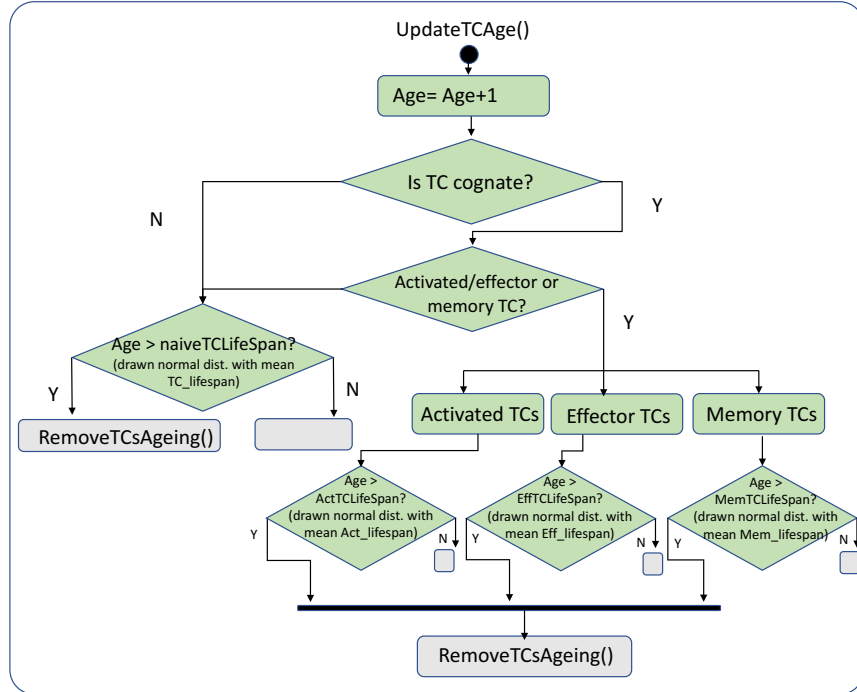


Figure S10. UML diagram for 'UpdateTCsAgeing'.

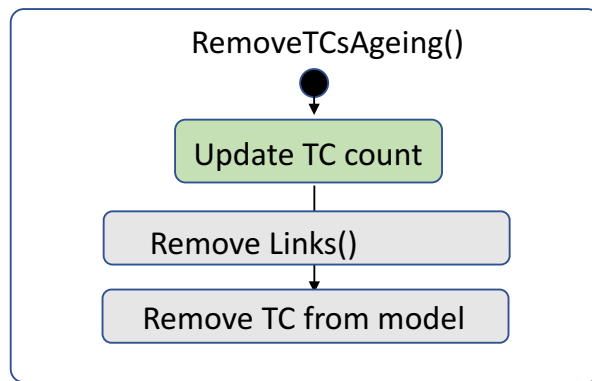


Figure S11. UML diagram for 'RemoveTCsAgeing'. The different types of TCs draw ages from gaussian distributions with a different mean value.

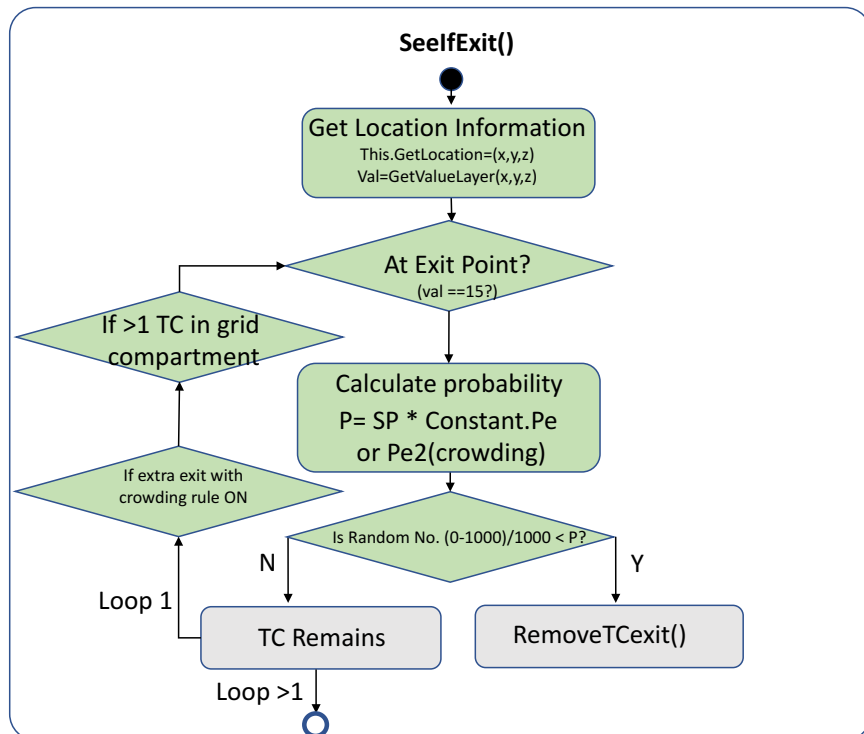


Figure S12. UML diagram for 'SeeIfExit'. The original simulations did not incorporate the second check of TC crowding (crowding rule).

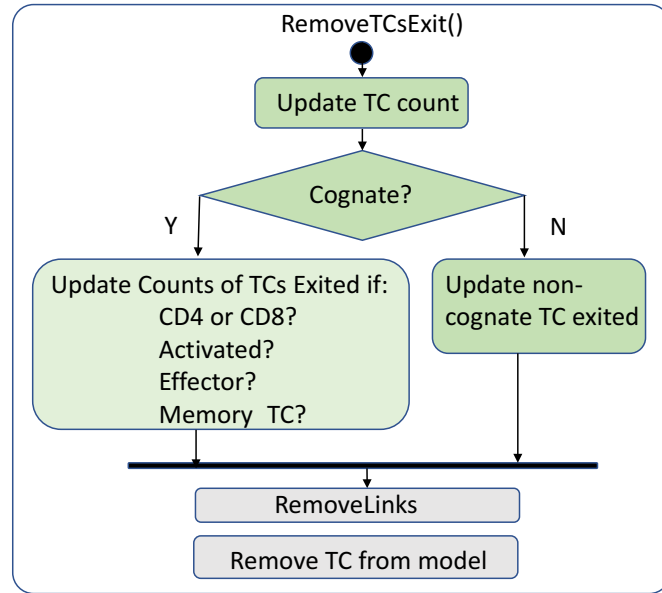


Figure S13. UML diagram for 'RemoveTCExit'. Ageing and TC exit are treated differently due to different counters being updated

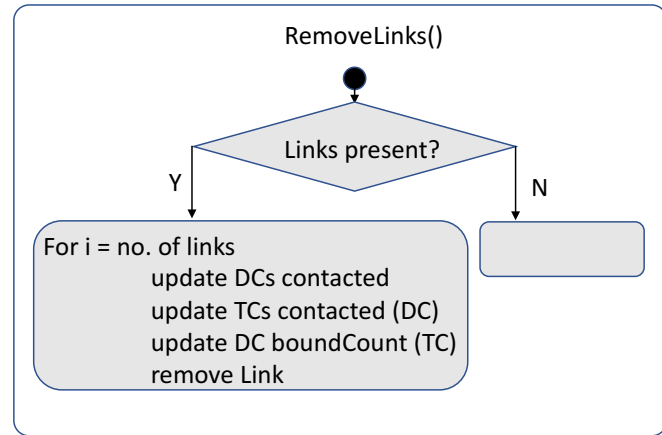


Figure S14. UML diagram for 'RemoveLinks'. Links between TCs and DCs are formed using a projection network, a feature of RepastSimphony, and must be removed when the connection is over.

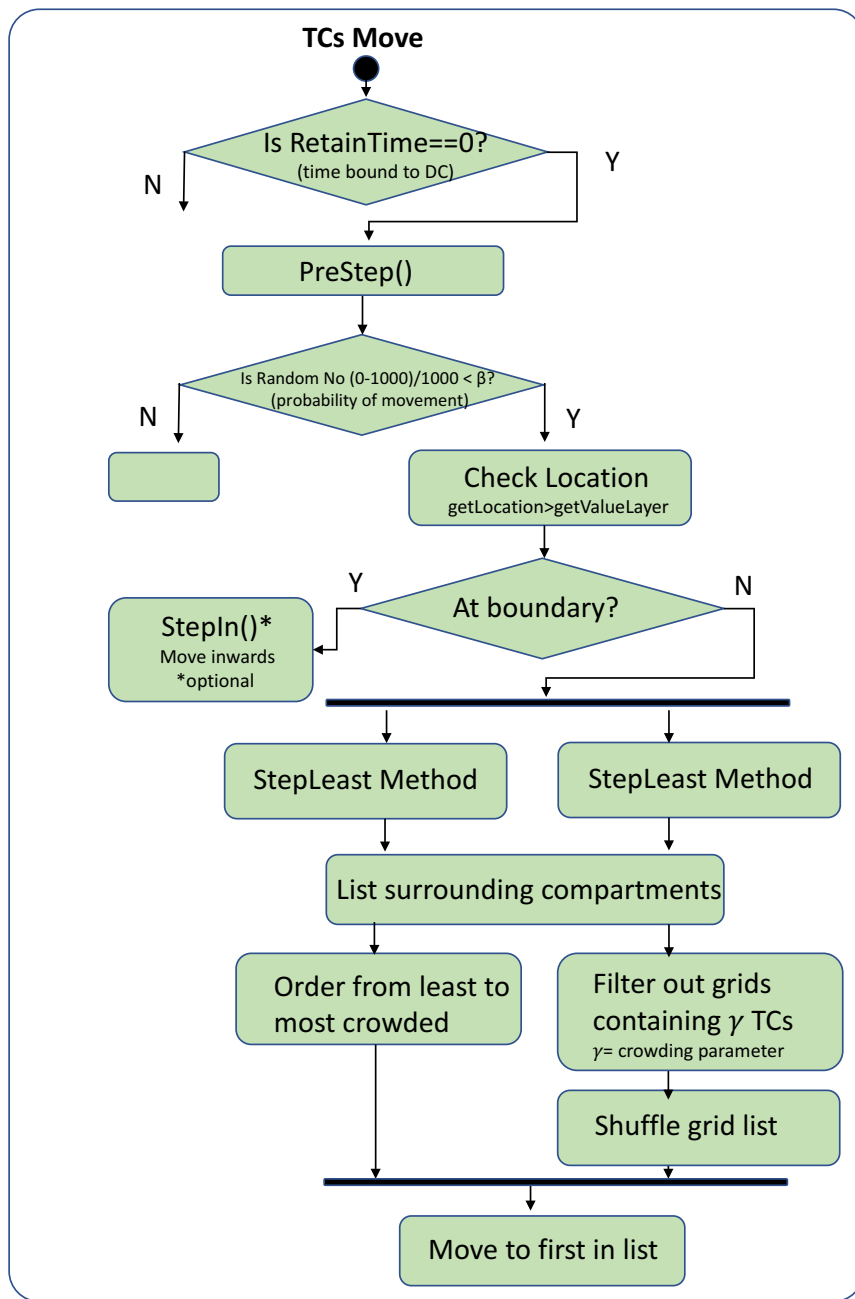


Figure S15. UML diagram for 'TCsMove'. The model has the capacity for different movement options, and maximum TCs per grid is set with crowding parameter γ

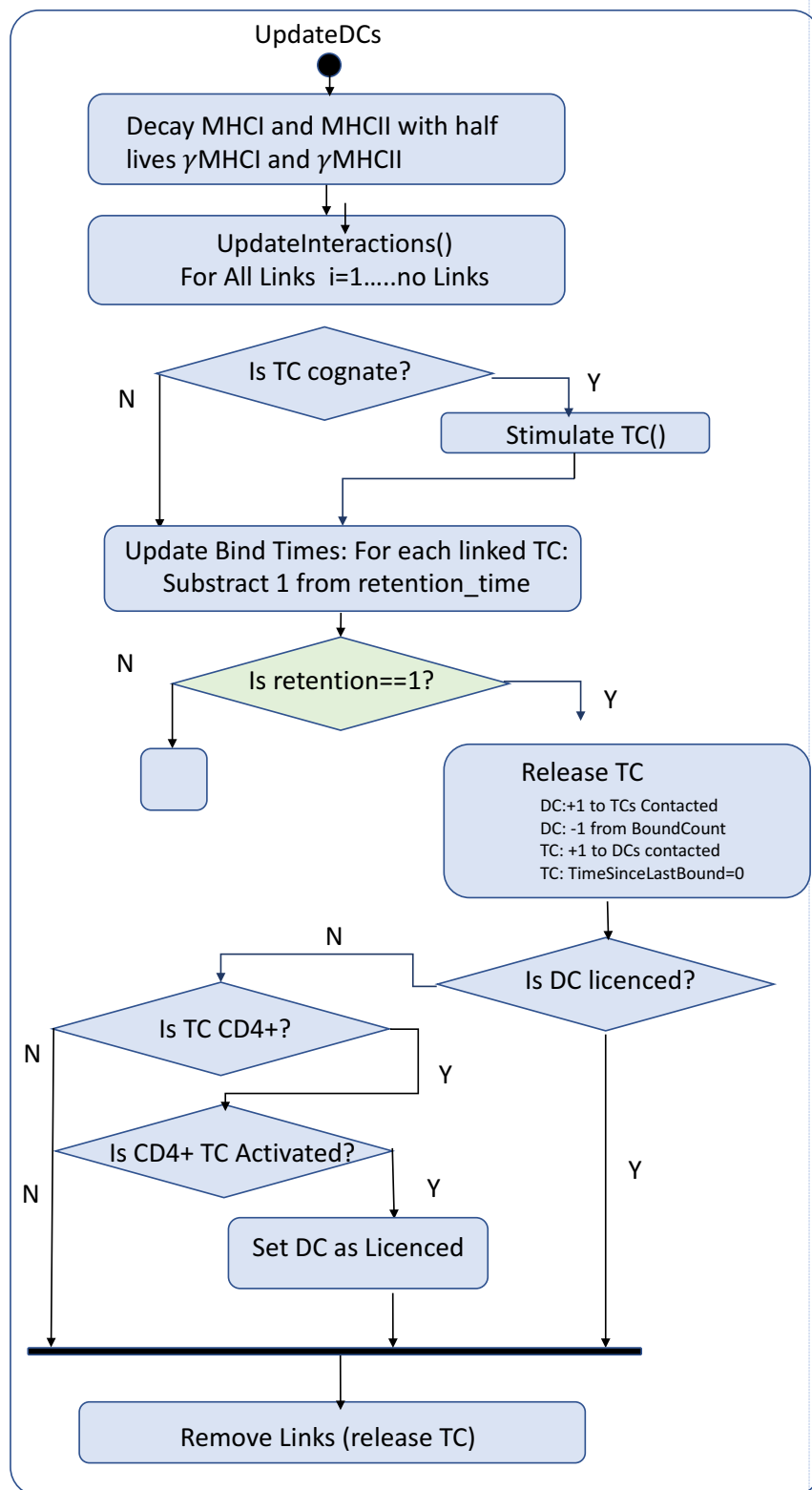


Figure S16. UML diagram for 'UpdateDCs'. DCs enter as mature migrating DCs but may become licenced through interaction with activated CD4+ TCs

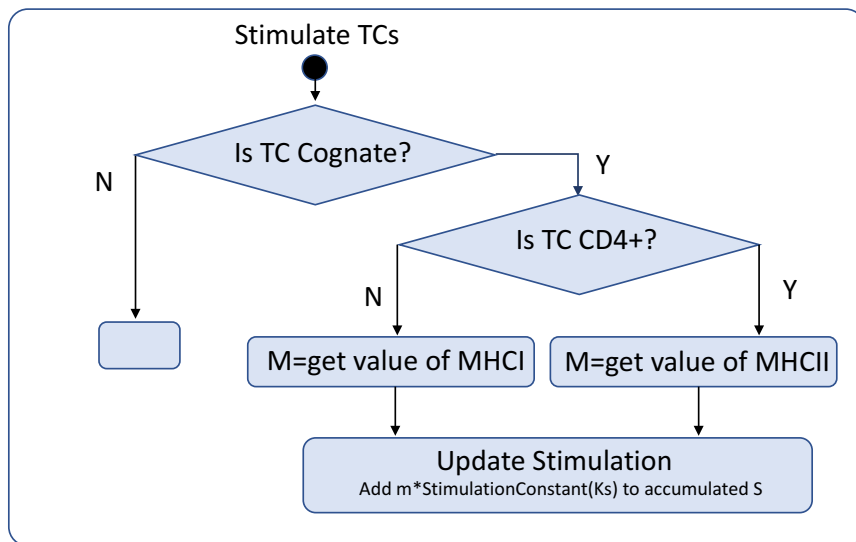


Figure S17. UML diagram for 'StimulateTCs'. DCs can access the variables of the agent attached via a projection link and thus alter their state based on the DCs MHC I/II presentation and the Stimulation constant, Ks.

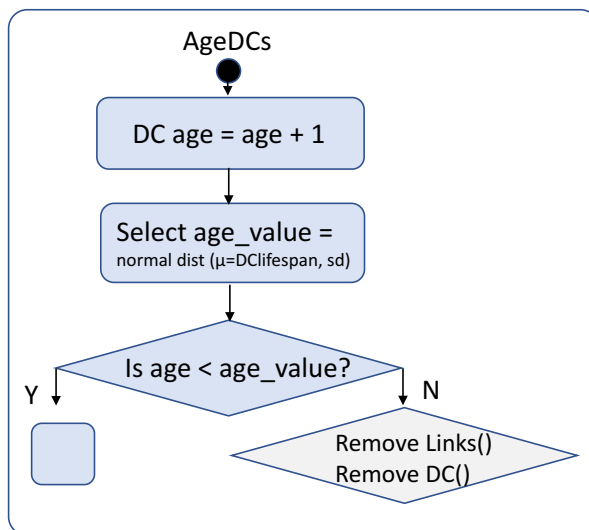


Figure S18. UML diagram for 'AgeDCs'. Mature DCs have a lifespan of around 2.5 days.

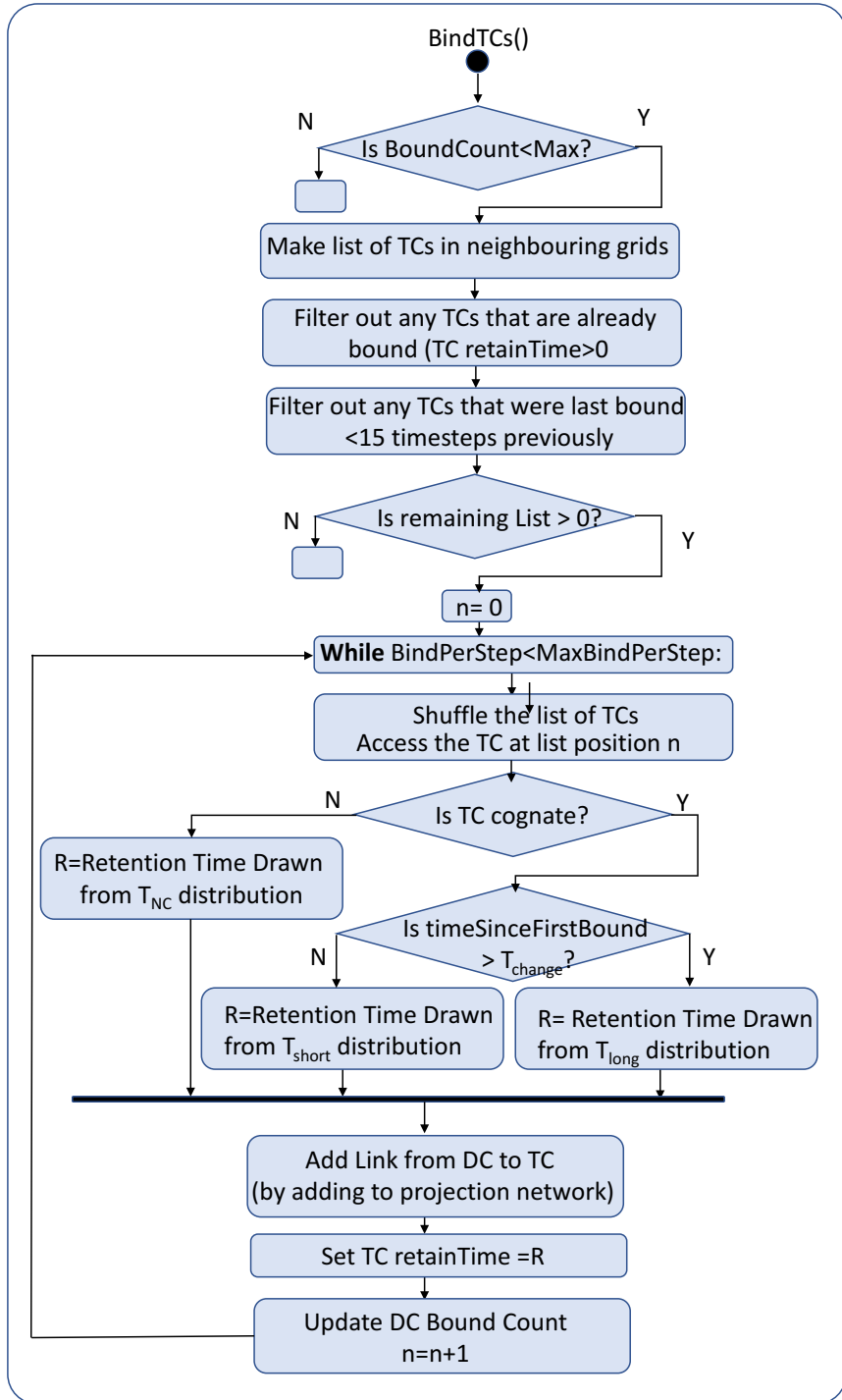
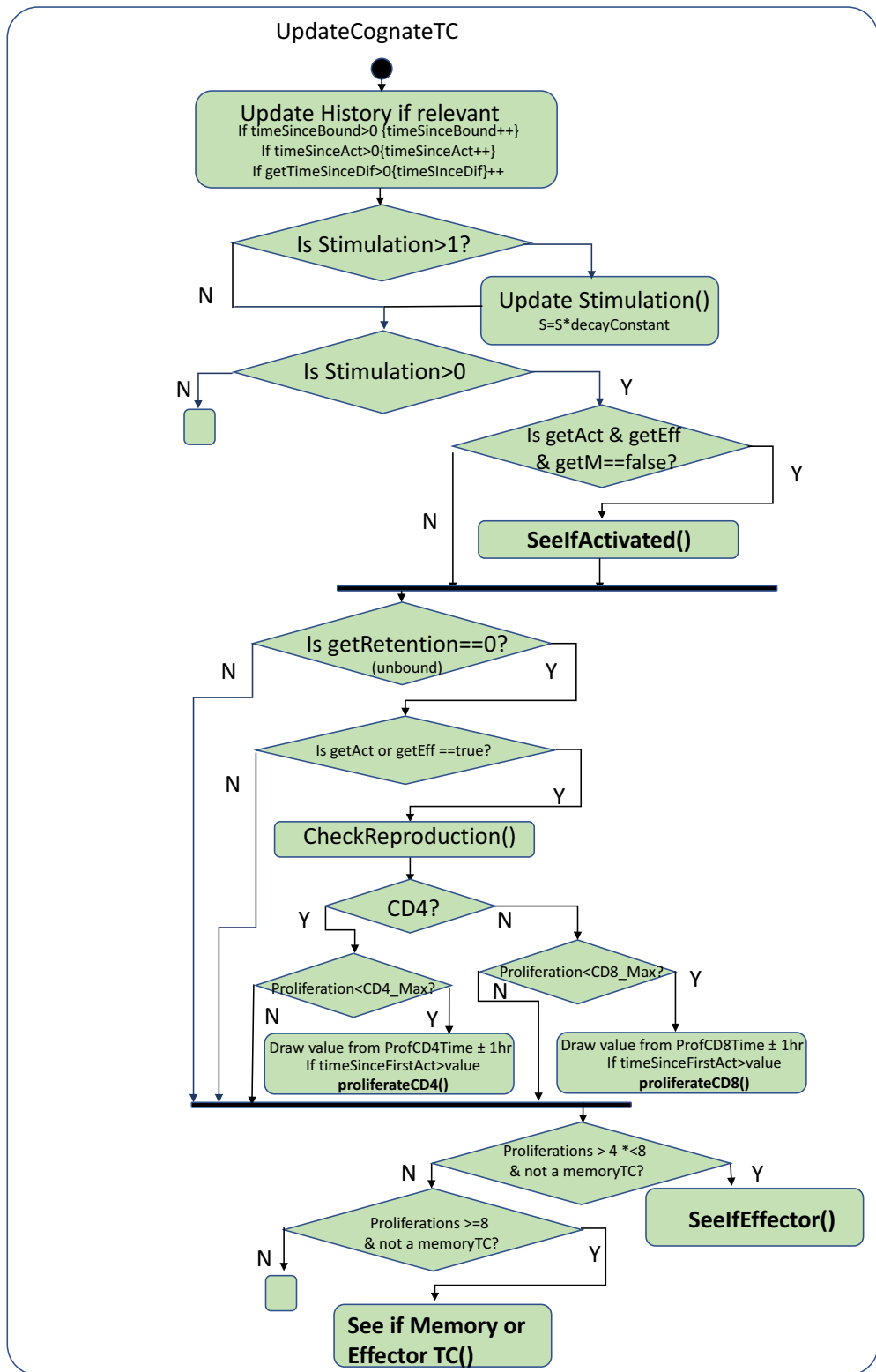


Figure S19. UML diagram for 'BindTCs'. TCs receive a 'interaction time' drawn from a relevant probability density function, based on their type and history.

**Figure S20.** UML diagram for 'UpdateCognateTCs'.

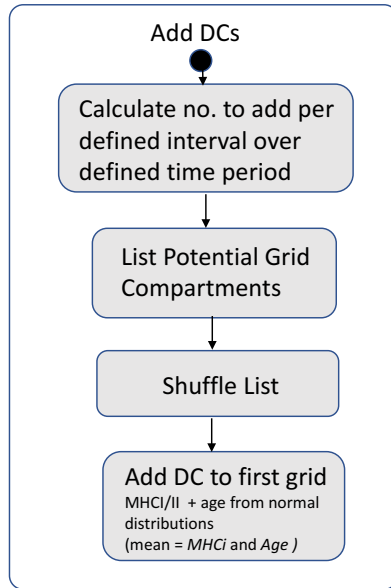


Figure S21. UML diagram for 'AddDCs'.

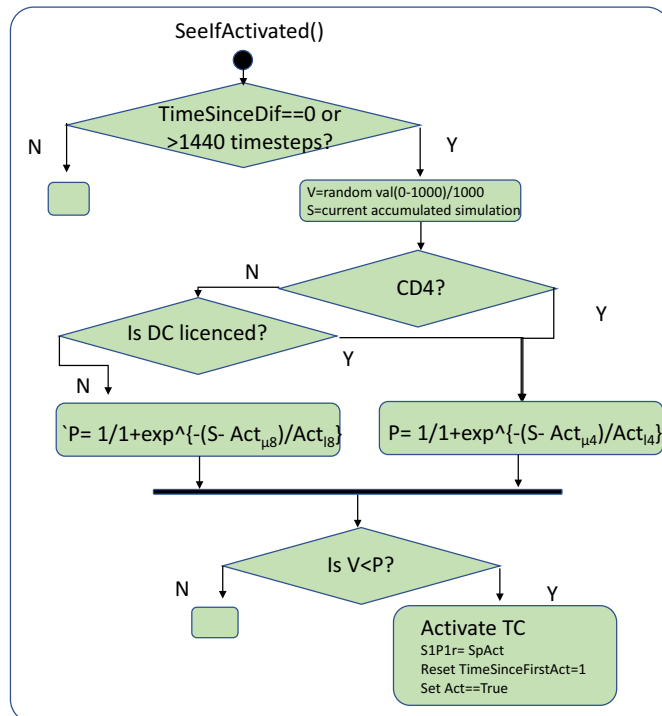
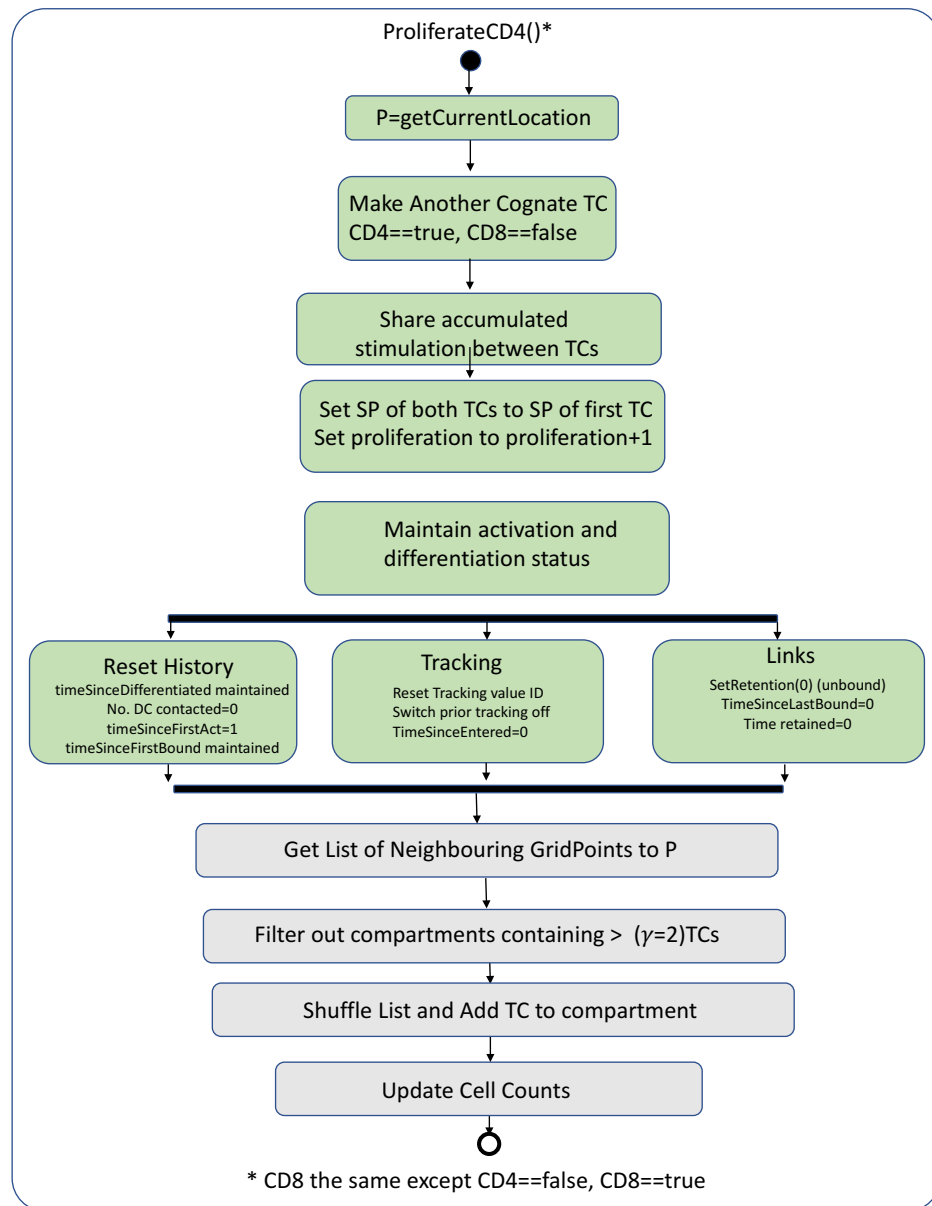


Figure S22. UML diagram for 'SeeIfActivated'.

**Figure S23.** UML diagram for 'Proliferation'.

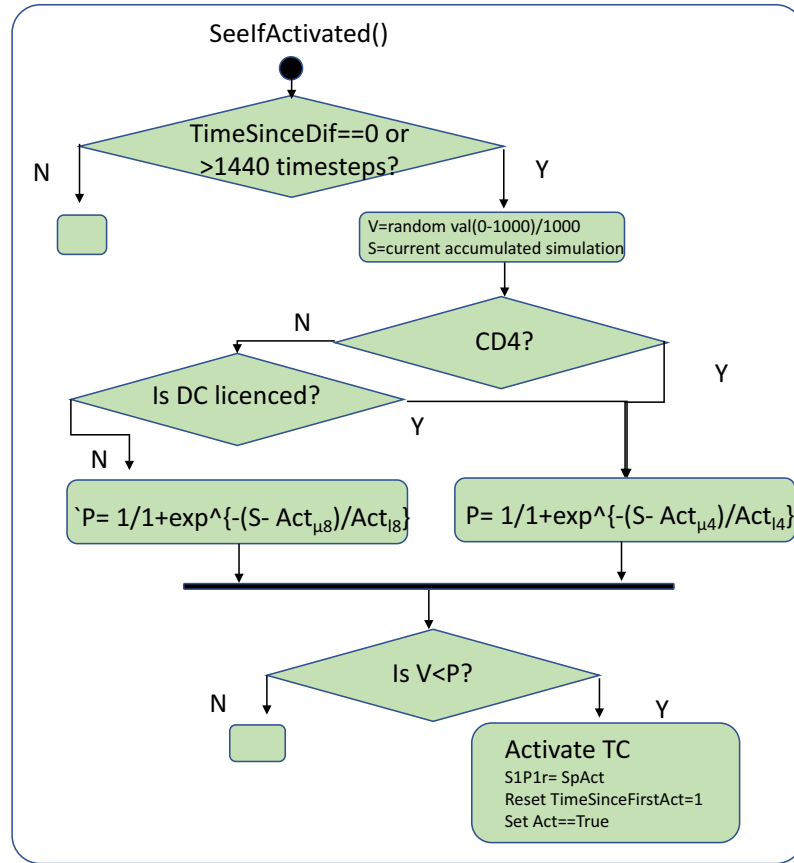


Figure S24. UML diagram for 'SeeIfEffector' or 'SeeIfEffectorMemory'. The two behaviours are similar but for seeIfEffectorMemory, the time since differentiation cannot be zero, as the TC must have previously differentiated, and more memory TCs are made.

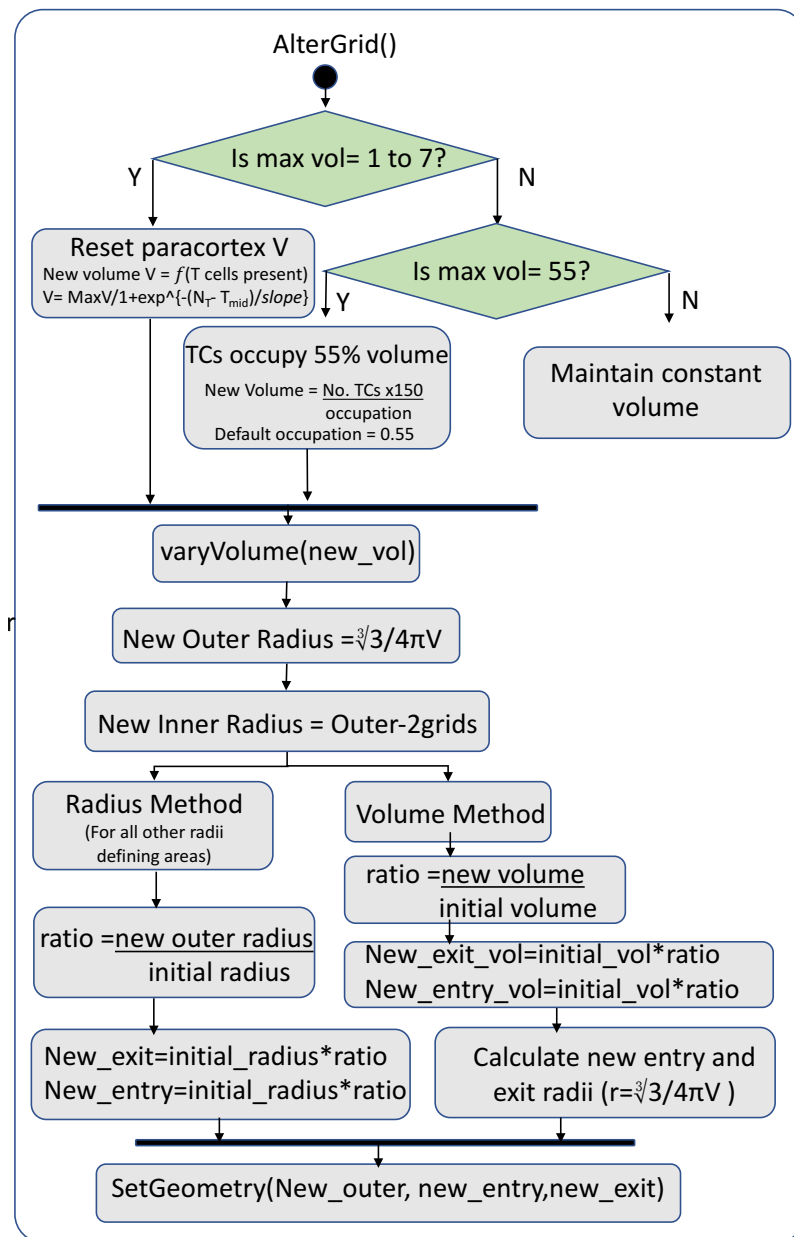


Figure S25. UML diagram for 'AlterGrid'. This methods carries out the calculation of the new paracortex volume then passes the calculated radii to 'Set Geometry'.

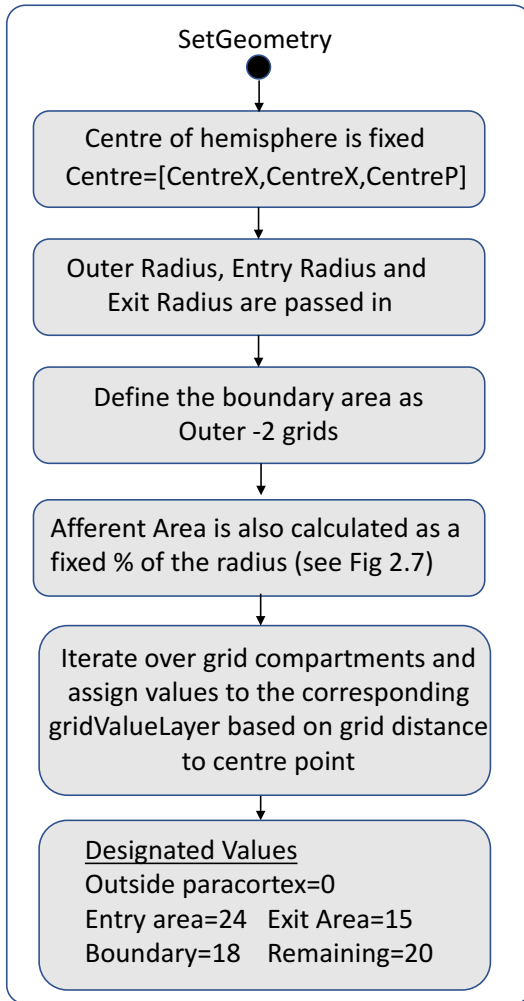


Figure S26. UML diagram for 'SetGeometry'. Only the radii are required as inputs to determine the geometry of the LN

2.0.2 citations for Parameter tables

Mueller and Germain (2009); Kuka and Iannaccone (2014) He (1985) Mueller and Germain (2009); Kuka and Iannaccone (2014) Tough and Sprent (1995) Sprent and Tough (2001) Smith et al. (1970); Hall and Morris (1965)

Nitschké et al. (2012); Paharkova-Vatchkova et al. (2004)

Acton et al. (2014); Kamath et al. (2002); Bousso (2008)

Park et al. (2010); Boscacci et al. (2010); Park et al. (2012); Girard et al. (2012); Miller et al. (2002)

Catron et al. (2004); Tomura et al. (2008)

Bajénoff et al. (2003); Yoon et al. (2007); Lawrence and Braciale (2004); Demotz et al. (1990); Lee et al. (2002); Arens and Schoenberger (2010)

Bajénoff et al. (2003); Yoon et al. (2007); Lawrence and Braciale (2004); Demotz et al. (1990); Lee et al. (2002); Arens and Schoenberger (2010)

Bajénoff et al. (2003); Yoon et al. (2007); Lawrence and Braciale (2004); Demotz et al. (1990); Lee et al. (2002); Arens and Schoenberger (2010)

Bajénoff et al. (2003); Yoon et al. (2007); Lawrence and Braciale (2004); Demotz et al. (1990); Lee et al. (2002); Arens and Schoenberger (2010)

De Boer et al. (2003); Nelson et al. (2015); Foulds et al. (2002); Tubo et al. (2013)

De Boer et al. (2003); Foulds et al. (2002)

Butz and Bevan (1998); Murali-Krishna et al. (1998); Busch et al. (1998); van Stipdonk et al. (2001)

Nelson et al. (2015); Tubo et al. (2013); Foulds et al. (2002)

Williams and Bevan (2004)

Williams and Bevan (2004)

Bousso (2008); Miller et al. (2004)

Bousso (2008); Miller et al. (2004); Mempel et al. (2004)

von Andrian and Mackay (2000); Hugues et al. (2004); Mempel et al. (2004); Stoll et al. (2002)

von Andrian and Mackay (2000); Hugues et al. (2004); Mempel et al. (2004); Stoll et al. (2002)

Bousso and Robey (2003)

Cella et al. (1999); Kukutsch et al. (2000); Cella et al. (1997); Baumgartner et al. (2010)

Cella et al. (1999); Kukutsch et al. (2000)

Cella et al. (1997); Baumgartner et al. (2010)

Laouini et al. (2000); Blattman et al. (2002); Nelson et al. (2015); Jenkins and Moon (2012)

Acton et al. (2014)

Acton et al. (2014)

Pham et al. (2008); Matloubian et al. (2004); Lo et al. (2005)

Pham et al. (2008); Matloubian et al. (2004); Lo et al. (2005); Garris et al. (2014)

Garris et al. (2014); Pham et al. (2008)

Garris et al. (2014); Pham et al. (2008)

Garris et al. (2014); Pham et al. (2008)

Hay and Hobbs (1977); Drayson and Smith (1981); Mackay et al. (1992); Webster et al. (2006)

Hay and Hobbs (1977); Drayson and Smith (1981); Mackay et al. (1992); Webster et al. (2006)

Hay and Hobbs (1977); Drayson and Smith (1981); Mackay et al. (1992); Webster et al. (2006)

REFERENCES

- Acton, S. E., Farrugia, A. J., Astarita, J. L., Mourao-Sa, D., Jenkins, R. P., Nye, E., et al. (2014). Dendritic cells control fibroblastic reticular network tension and lymph node expansion. *Nature* 514, 498–502
- Arens, R. and Schoenberger, S. P. (2010). Plasticity in programming of effector and memory cd8(+) t-cell formation. *Immunological reviews* 235, 190–205
- Bajénoff, M., Granjeaud, S., and Guerder, S. (2003). The strategy of t cell antigen-presenting cell encounter in antigen-draining lymph nodes revealed by imaging of initial t cell activation. *Journal of Experimental Med* 198, 715–724. doi:10.1084/jem.20030167
- Battaglia, A., Ferrandina, G., Buzzonetti, A., Malinconico, P., Legge, F., Salutari, V., et al. (2003). Lymphocyte populations in human lymph nodes. alterations in cd4(+) cd25(+) t regulatory cell phenotype and t-cell receptor beta-repertoire. *Immunology* 110, 304–312
- Baumgartner, C., Ferrante, A., Nagaoka, M., Gorski, J., and Malherbe, L. P. (2010). Peptide-mhc class ii complex stability governs cd4 t cell clonal selection. *Journal of immunology (Baltimore, Md. : 1950)* 184, 573–581
- Blattman, J. N., Antia, R., Sourdive, D. J., Wang, X., Kaech, S. M., Murali-Krishna, K., et al. (2002). Estimating the precursor frequency of naive antigen-specific cd8 t cells. *The Journal of Experimental Medicine* 195, 657–664
- Bogle, G. and Dunbar, P. R. (2008). Simulating t-cell motility in the lymph node paracortex with a packed lattice geometry. *Imm Cell Biol* 86, 676–687
- Boscacci, R., Pfeiffer, F., Gollmer, K., and Sevilla, A. (2010). Comprehensive analysis of lymph node stroma-expressed ig superfamily members reveals redundant and nonredundant roles for ICAM-1, ICAM-2, and VCAM-1 in lymphocyte homing. *Blood* 116, 915–25
- Bousso, P. (2008). T-cell activation by dendritic cells in the lymph node: lessons from the movies. *Nature Reviews Immunology* 8, 675–84
- Bousso, P. and Robey, E. (2003). Dynamics of CD8+ t cell priming by dendritic cells in intact lymph nodes. *Nature immunology* 4, 579–585
- Brown, L. V., Gaffney, E. A., Wagg, J., and Coles, M. C. (2018). An in silico model of cytotoxic t-lymphocyte activation in the lymph node following short peptide vaccination. *Journal of the Royal Society, Interface* 15, 2018.0041
- Busch, D. H., Pilip, I. M., Vijh, S., and Pamer, E. G. (1998). Coordinate regulation of complex t cell populations responding to bacterial infection. *Immunity* 8, 353–362
- Butz, E. A. and Bevan, M. J. (1998). Massive expansion of antigen-specific cd8(+) t cells during an acute virus infection. *Immunity* 8, 167–175
- Cahill, R., Frost, H., and Trnka, Z. (1976). The effects of antigen on the migration of recirculating lymphocytes through single lymph nodes. *J. Exp. Med.* 143, 870–888. doi:10.1084/jem.143.4.870
- Catron, D. M., Itano, A. A., Pape, K. A., Mueller, D. L., and Jenkins, M. K. (2004). Visualizing the first 50 hr of the primary immune response to a soluble antigen. *Immunity*. 21, 341–347
- Cella, M., Engering, A., Pinet, V., Pieters, J., and Lanzavecchia, A. (1997). Inflammatory stimuli induce accumulation of mhc class ii complexes on dendritic cells. *Nature* 388, 782–7
- Cella, M., Salio, M., Sakakibara, Y., Langen, H., Julkunen, I., and Lanzavecchia, A. (1999). Maturation, activation, and protection of dendritic cells induced by double-stranded rna. *The Journal of Experimental Medicine* 189, 821–829
- Celli, S., Day, M., Müller, A. J., Molina-Paris, C., Lythe, G., and Bousso, P. (2012). How many dendritic cells are required to initiate a t-cell response? *Blood* 120, 3945–3948. doi:10.1182/blood-2012-01-408260

- De Boer, R. J., Homann, D., and Perelson, A. S. (2003). Different dynamics of cd4+ and cd8+ t cell responses during and after acute lymphocytic choriomeningitis virus infection. *The Journal of Immunology* 171, 3928–3935. doi:10.4049/jimmunol.171.8.3928
- Demotz, S., Grey, H., and Sette, A. (1990). The minimal number of class ii mhc-antigen complexes needed for t cell activation. *Science* 249, 1028–1030. doi:10.1126/science.2118680
- Drayson, M. T. and Smith, M. E. (1981). The sequence of changes in blood flow and lymphocyte influx to stimulated rat lymph nodes. *Immunology* 44, 125–133
- Foulds, K. E., Zenewicz, L. A., Shedlock, D. J., Jiang, J., Troy, A. E., and Shen, H. (2002). Cutting edge: Cd4 and cd8 t cells are intrinsically different in their proliferative responses. *The Journal of Immunology* 168, 1528–1532. doi:10.4049/jimmunol.168.4.1528
- Garris, C. S., Blaho, V. A., Hla, T., and Han, M. H. (2014). Sphingosine-1-phosphate receptor 1 signalling in t cells: trafficking and beyond. *Immunology* 142, 347–353
- Germain, R. N. and Stefanová, I. (1999). The dynamics of t cell receptor signaling: Complex orchestration and the key roles of tempo and cooperation. *Annual Review of Immunology* 17, 467–522. doi:10.1146/annurev.immunol.17.1.467
- Girard, J. P., Moussion, C., and Förster, R. (2012). HEVs, lymphatics and homeostatic immune cell trafficking in lymph nodes. *Nat. Rev. Immunol.* 12, 762–73. doi:10.1038/nri3298
- Habenicht, L. M., Albershardt, T. C., Iritani, B. M., and Ruddell, A. (2016). Distinct mechanisms of b and t lymphocyte accumulation generate tumor-draining lymph node hypertrophy. *Oncobiology* 5, e1204505
- Hall, J. and Morris, B. (1965). The immediate effect of antigens on the cell output of a lymph node. *British journal of experimental pathology*
- Harris, T. H., Banigan, E. J., Christian, D. A., Konradt, C., Tait Wojno, E. D., Norose, K., et al. (2012). Generalized lévy walks and the role of chemokines in migration of effector cd8+ t cells. *Nature* 486, 545 EP –
- Hay, J. B. and Hobbs, B. B. (1977). The flow of blood to lymph nodes and its relation to lymphocyte traffic and the immune response. *Journal of Experimental Medicine* 145, 31–44
- He, Y. (1985). Scanning electron microscope studies of the rat mesenteric lymph node with special reference to high-endothelial venules and hitherto unknown lymphatic labyrinth. *Archivum histologicum Japonicum*, 1–15
- Hugues, S., Fetler, L., Bonifaz, L., Helft, J., Amblard, F., and Amigorena, S. (2004). Distinct t cell dynamics in lymph nodes during the induction of tolerance and immunity. *Nature Immunology* 5, 1235–42
- Jenkins, M. K. and Moon, J. J. (2012). The role of naïve t cell precursor frequency and recruitment in dictating immune response magnitude. *Journal of Immunology (Baltimore, Md. : 1950)* 188, 4135–4140
- Kaech, S. M. and Ahmed, R. (2001). Memory cd8+ t cell differentiation: initial antigen encounter triggers a developmental program in naïve cells. *Nature Immunology* 2, 415–22
- Kamath, A. T., Henri, S., Battye, F., Tough, D. F., and Shortman, K. (2002). Developmental kinetics and lifespan of dendritic cells in mouse lymphoid organs. *Blood* 100, 1734–1741
- Kuka, M. and Iannacone, M. (2014). The role of lymph node sinus macrophages in host defense. *Annals of the New York Academy of Sciences* 1319, 38–46. doi:10.1111/nyas.12387
- Kukutsch, N. A., Rossner, S., Austyn, J. M., Schuler, G., and Lutz, M. B. (2000). Formation and kinetics of mhc class i-ovalbumin peptide complexes on immature and mature murine dendritic cells. *Journal of Investigative Dermatology* 115, 449 – 453. doi:<https://doi.org/10.1046/j.1523-1747.2000.00084.x>

- Lanzavecchia, A. and Sallusto, F. (2002). Progressive differentiation and selection of the fittest in the immune response. *Nature Reviews Immunology* 2, 982–7
- Laouini, D., Casrouge, A., Dalle, S., Lemonnier, F., Kourilsky, P., and Kanellopoulos, J. (2000). Vi2 t cell repertoire of cd8+ splenocytes selected on nonpolymorphic mhc class i molecules. *The Journal of Immunology* 165, 6381–6386. doi:10.4049/jimmunol.165.11.6381
- Lawrence, C. W. and Braciale, T. J. (2004). Activation, differentiation, and migration of naive virus-specific cd8+ t cells during pulmonary influenza virus infection. *The Journal of Immunology* 173, 1209–1218. doi:10.4049/jimmunol.173.2.1209
- Lee, W. T., Pasos, G., Cecchini, L., and Mittler, J. N. (2002). Continued antigen stimulation is not required during cd4+ t cell clonal expansion. *The Journal of Immunology* 168, 1682–1689. doi:10.4049/jimmunol.168.4.1682
- Linderman, J. J., Riggs, T., Pande, M., Miller, M., Marino, S., and Kirschner, D. E. (2010). Characterizing the dynamics of cd4+ t cell priming within a lymph node. *The Journal of Immunology* 184, 2873–2885. doi:10.4049/jimmunol.0903117
- Lo, C., Xu, Y., Proia, R., and Cyster, J. (2005). Cyclical modulation of sphingosine-1-phosphate receptor 1 surface expression during lymphocyte recirculation and relationship to lymphoid organ transit. *Journal of Experimental Medicine* 2, 291–301. doi:10.1084/jem.20041509
- Mackay, C., Marston, W., and Dudler, L. (1992). Altered patterns of t cell migration through lymph nodes and skin following antigen challenge. *European journal of Imm.* 22, 2205–10. doi:10.1002/eji.1830220904
- Matloubian, M., Lo, C., Cinamon, G., Lesneski, M., and Xu, Y. (2004). Lymphocyte egress from thymus and peripheral lymphoid organs is dependent on S1P receptor 1. *Nature* 427, 355–60. doi:10.1038/nature02284
- Mempel, T. R., Henrickson, S. E., and Von Andrian, U. H. (2004). T-cell priming by dendritic cells in lymph nodes occurs in three distinct phases. *Nature* 427, 154–9. doi:10.1038/nature02238
- Miller, M. J., Hejazi, A. S., Wei, S. H., Cahalan, M. D., and Parker, I. (2004). T cell repertoire scanning is promoted by dynamic dendritic cell behavior and random t cell motility in the lymph node. *Proc. Natl. Acad. Sci. U.S.A.* 101, 998–1003. doi:10.1073/pnas.0306407101
- Miller, M. J., Wei, S. H., Parker, I., and Cahalan, M. D. (2002). Two-photon imaging of lymphocyte motility and antigen response in intact lymph node. *Science* 296, 1869–73. doi:10.1126/science.1070051
- Mueller, S. N. and Germain, R. N. (2009). Stromal cell contributions to the homeostasis and functionality of the immune system. *Nature Reviews Immunology* 9, 618–29
- Murali-Krishna, K., Altman, J. D., Suresh, M., Sourdive, D. J. D., Zajac, A. J., Miller, J. D., et al. (1998). Counting antigen-specific cd8 t cells: A reevaluation of bystander activation during viral infection. *Immunity* 8, 177–187
- Nelson, R. W., Beisang, D., Tubo, N. J., Dileepan, T., Wiesner, D. L., Nielsen, K., et al. (2015). T cell receptor cross-reactivity between similar foreign and self peptides influences naïve cell population size and autoimmunity. *Immunity* 42, 95–107
- Nitschké, M., Aeberle, D., Abadier, M., Haener, S., Lucic, M., Vigl, B., et al. (2012). Differential requirement for rock in dendritic cell migration within lymphatic capillaries in steady-state and inflammation. *Blood* 120, 2249–2258. doi:10.1182/blood-2012-03-417923
- Paharkova-Vatchkova, V., Maldonado, R., and Kovats, S. (2004). Estrogen preferentially promotes the differentiation of cd11c+ cd11bintermediate dendritic cells from bone marrow precursors. *The Journal of Immunology* 172, 1426–1436. doi:10.4049/jimmunol.172.3.1426

- Park, C., Hwang, I., Sinha, R., and Kamenyeva, O. (2012). Lymph node b lymphocyte trafficking is constrained by anatomy and highly dependent upon chemo-attractant desensitization. *Blood* 119, 978–989
- Park, E., Peixoto, A., Imai, Y., Goodarzi, A., and Cheng, G. (2010). Distinct roles for LFA-1 affinity regulation during t-cell adhesion, diapedesis, and interstitial migration in lymph nodes. *Blood* 115, 1572–81
- Pham, T., Okada, T., Matloubian, M., Lo, C., and Cyster, J. (2008). S1P 1 receptor signaling overrides retention mediated by gi-coupled receptors to promote t cell egress. *Immunity* 28, 122–133
- Rachmilewitz, J. and Lanzavecchia, A. (2002). A temporal and spatial summation model for t-cell activation: signal integration and antigen decoding. *Trends in Immunology* 23, 592–595. doi:[https://doi.org/10.1016/S1471-4906\(02\)02342-6](https://doi.org/10.1016/S1471-4906(02)02342-6)
- Schrum, A. G., Palmer, E., and Turka, L. A. (2005). Distinct temporal programming of naive cd4(+) t cells for cell division versus tcr-dependent death susceptibility by antigen-presenting macrophages. *European journal of immunology* 35, 449–459
- Shaulov, A. and Murali-Krishna, K. (2008). Cd8 t cell expansion and memory differentiation are facilitated by simultaneous and sustained exposure to antigenic and inflammatory milieu. *The Journal of Immunology* 180, 1131–1138. doi:10.4049/jimmunol.180.2.1131
- Smith, J. B., McIntosh, G. H., and Morris, B. (1970). The traffic of cells through tissues: a study of peripheral lymph in sheep. *Journal of Anatomy* 107, 87–100
- Sprent, J. and Tough, D. F. (2001). T cell death and memory. *Science* 293, 245–248. doi:10.1126/science.1062416
- Stoll, S., Delon, J., Brotz, T., and Germain, R. (2002). Dynamic imaging of t cell-dendritic cell interactions in lymph nodes. *Science* 296, 1873–6. doi:10.1126/science.1071065
- Tomura, M., Yoshida, N., and Tanaka, J. (2008). Monitoring cellular movement in vivo with photoconvertible fluorescence protein 'kaede' transgenic mice. *PNAS* 105, 10871–6. doi:10.1073/pnas.0802278105
- Tough, D. F. and Sprent, J. (1995). Life span of naive and memory t cells. *STEM CELLS* 13, 242–249. doi:10.1002/stem.5530130305
- Tubo, N. J., Pagán, A. J., Taylor, J. J., Nelson, R. W., Linehan, J. L., Ertelt, J. M., et al. (2013). Single naive cd4⁺ t cells from a diverse repertoire produce different effector cell types during infection. *Cell* 153, 785–796
- van Stipdonk, M. J. B., Lemmens, E. E., and Schoenberger, S. P. (2001). Naïve ctls require a single brief period of antigenic stimulation for clonal expansion and differentiation. *Nature Immunology* 2, 423–9
- von Andrian, U. and Mackay, C. (2000). T-cell function and migration, two sides of the same coin. *New England Journal of Medicine* 343, 1020–34
- Webster, B., Ekland, E. H., Agle, L. M., Chyou, S., Ruggieri, R., and Lu, T. T. (2006). Regulation of lymph node vascular growth by dendritic cells. *J. Exp. Med.* 203, 1903–13. doi:10.1084/jem.20052272
- Williams, M. A. and Bevan, M. J. (2004). Shortening the infectious period does not alter expansion of cd8 t cells but diminishes their capacity to differentiate into memory cells. *The Journal of Immunology* 173, 6694–6702. doi:10.4049/jimmunol.173.11.6694
- Wong, P. and Pamer, E. G. (2001). Cutting edge: Antigen-independent cd8 t cell proliferation. *The Journal of Immunology* 166, 5864–5868. doi:10.4049/jimmunol.166.10.5864
- Yoon, H., Legge, K. L., Sung, S.-s. J., and Braciale, T. J. (2007). Sequential activation of cd8+ t cells in the draining lymph nodes in response to pulmonary virus infection. *The Journal of Immunology* 179, 391–399. doi:10.4049/jimmunol.179.1.391